Manipulation of microparticles in colloidal liquids by *Z*-scan-based optical trapping

Jin Liu,[1] Qiao-Feng Dai,[1] Tian-Hua Feng,[1] Hai-Ying Liu,[1] Li-Jun Wu,[1] Qi Guo,[1] Wei Hu,[1] Song-Hao Liu,[1] Sheng Lan,[1,a)] Achanta Venu Gopal,[2] and Vyacheslav A. Trofimov[3]
[1]*Laboratory of Photonic Information Technology, School for Information and Optoelectronic Science and Engineering, South China Normal University, Guangzhou, Guangdong 510006, People's Republic of China*
[2]*DCMP and MS, Tata Institute of Fundamental Research, Homi Bhabha Road, Mumbai 400005, India*
[3]*Department of Computational Mathematics and Cybernetics, M. V. Lomonosov Moscow State University, Moscow 119992, Russia*

(Received 25 July 2008; accepted 22 October 2008; published online 8 December 2008)

Manipulation of microparticles in colloidal liquids by using *Z*-scan-based optical trapping is systematically investigated. A physical model for the creation and annihilation of ordered structures in *Z*-scan-based optical trapping is presented theoretically and verified experimentally. Disordered, ordered, and intermediate states appearing in *Z*-scan trapping experiments are discussed and the conditions for realizing phase transition and observing self-induced transparency are clarified. We experimentally demonstrate the high quality and good stability of the formed structures, the sequential trapping of individual microparticles, and the multiple trapping processes. The dependence of the quality of the formed structures on trapping power, scanning speed, and the size and material of microparticles are identified. © *2008 American Institute of Physics*.
[DOI: 10.1063/1.3039454]

I. INTRODUCTION

Since the pioneering work of Ashkin *et al.*[1,2] in 1970 and 1986, the trapping and manipulation of particles has received intensive and extensive studies in the past two decades. With the understanding of the physical mechanism and the development of trapping technique, the research in this field has been extended from single particles[2] to a large number of particles,[3] from microparticles[2] to nanoparticles,[4,5] from spherical particles[2] to those with various shapes,[6,7] and from polymer particles[2] to metal[8,9] and semiconductor particles,[10] among others. Particularly, much effort has been devoted to the trapping and manipulation of a large number of particles with the hope of building ordered structures with dynamic and reversible features. These ordered structures, which are generated and held by photons, are generally referred to as optical matters.[11–14] In principle, they possess all of the physical properties of photonic crystals[15,16] that have been widely studied and explored for the construction of various functional devices.[17,18] Moreover, their dynamic and reversible features make them quite attractive from the viewpoints of fundamental research and device application. So far, the most popular techniques that are employed to generate ordered structures are based on holographic optics.[19–24] However, the experimental setups of the holographic techniques are usually complicated, and the ordered structures created by these techniques have not yet met the demands of practical device application. Therefore, it is necessary to develop a simple and effective method to assemble randomly distributed particles into ordered structures through optical trapping.

Very recently, we proposed a simple method for manipulating a large number of particles based on the combination of the single beam optical trapping[2] and the conventional *Z*-scan technique.[25,26] By using this method, we have demonstrated the phase transition from a disordered state to an ordered one and observed self-induced transparency phenomenon.[27] Although this technique has been confirmed to be an effective way of assembling randomly distributed particles into an ordered structure, many issues remain to be clarified, for instance, the influence of various parameters such as particle size and concentration, sample cell thickness, scanning speed, and trapping power on the quality and stability of the formed ordered structures. In this article, we present a systematic study on *Z*-scan-based optical trapping. The paper is organized as follows. In Sec. II, we illustrate by numerical simulation the physical model for the creation and annihilation of ordered structures in *Z*-scan-based optical trapping. Then, the disordered, ordered, and intermediate states found in the *Z*-scan trapping experiments are described in Sec. III. It is shown in Sec. IV that well reproduced ordered structures with high quality and good stability can be obtained in *Z*-scan trapping processes by optimizing the trapping conditions. In Sec. V, we clarify the basic requirements for achieving ordered structures and observing self-induced transparency. The sequential trapping of individual particles is described in Sec. VI. In Sec. VII, we demonstrate the achievement of ordered structures from a solution with low particle concentration by utilizing multiple trapping processes. The effects of scanning speed and trapping power on the quality of the ordered structures are clarified in Sec. VIII, while those of particle size and material are discussed in Sec. IX. Finally, we summarize our research works in Sec. X.

a)Author to whom correspondence should be addressed. Electronic mail: slan@scnu.edu.cn.

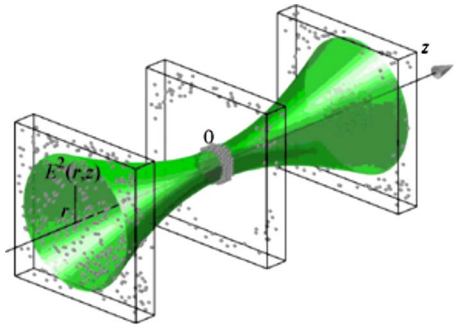

FIG. 1. (Color online) Schematic description of the principle for the creation of a close-packed array by *Z*-scan-based optical trapping process. The change in the particle concentration within the beam waist at three places (before, after, and at the focus point) is shown.

II. PHYSICAL MODEL AND EXPERIMENTAL SETUP FOR *Z*-SCAN-BASED OPTICAL TRAPPING

The physical picture for the creation and annihilation of ordered structures in *Z*-scan-based optical trapping is schematically illustrated in Fig. 1. It is well known that a laser beam acts as an optical potential well where microparticles are trapped due to the existence of gradient force. In general, the optical force exerted on an object can be expressed as[10]

$$\langle \mathbf{F} \rangle = \int_S \mathbf{T} \cdot \mathbf{n} dS, \tag{1}$$

where $\langle \mathbf{F} \rangle$ stands for the time average of the optical force, $\mathbf{T}$ is the Maxwell stress tensor, and $\mathbf{n}$ is the normal vector of the surface surrounding the object. For a focused Gaussian beam, it is convenient to introduce a coordinate system with two parameters r and z to describe the distribution of the electric field intensity $E^2(r,z)$, as shown in Fig. 1. For a small dielectric sphere suspended in a fluid, the gradient force and the potential energy are derived to be[13]

$$\langle \mathbf{F}(r,z) \rangle = \frac{1}{2} \frac{\varepsilon_1 - \varepsilon_2}{(\varepsilon_1/\varepsilon_2) + 2} a^3 \nabla E^2(r,z), \tag{2}$$

$$\langle W(r,z) \rangle = -\frac{1}{2} \frac{\varepsilon_1 - \varepsilon_2}{(\varepsilon_1/\varepsilon_2) + 2} a^3 E^2(r,z). \tag{3}$$

Here, a is the radius of the sphere and ε_i $(i=1,2)$ are the permittivities of the sphere and the fluid, respectively.

It is noticed from Eq. (3) that the width and the depth of the potential well are determined by the width and the intensity of the Gaussian beam. If the beam size is reduced slowly and continuously, then the width of the potential well will be accordingly narrowed while its depth will be significantly increased. As a result, the particles initially trapped by the potential well have nearly no chance to escape and their separation will become smaller and smaller. This process is equivalent to squeezing the water in between the particles out of the optical potential well, making them closer and closer. Finally, a regular lattice of the microparticles (e.g., close-packed array) that fully occupies the beam volume will be obtained provided that the number of the particles being trapped is adequate. Therefore, a transition of the trapping region from a disordered to an ordered structure can be realized by utilizing this method.

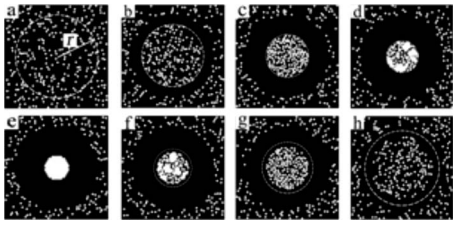

FIG. 2. Two-dimensional simulation of the distribution of PS spheres at different positions in a *Z*-scan-based trapping process. (a) Far from the focus point. (b) Optical trapping becomes effective. [(c) and (d)] Sample cell approaches the focus point. (e) Sample cell reaches the focus point. [(f)–(h)] Sample cell leaves the focus point.

The simulation of the movement of a large number of particles driven by optical force is a complicated issue. Apart from optical force, it is necessary to consider various effects on the motion of particles, including optical binding, hard-sphere repulsion, van der Waals force, Debye screening, etc. In addition, the diffusion of particles caused by Brownian motion that may act against optical trapping should also be taken into account. However, it is a big challenge to predict the motion of particles when all these factors are taken into account. Usually, it is assumed that one of them would play a crucial role in determining the movement or distribution of particles. For instance, Grzegorczyk *et al.*[28] calculated the effect of optical binding on the distribution of microparticles and they considered optical binding as a dominant effect.

To gain a deep insight into the formation of ordered structures from randomly distributed microparticles in *Z*-scan trapping processes, we have performed a two-dimensional simulation for the evolution of the distribution of microparticles with decreasing beam size, as shown in Fig. 2. In the simulation, it is assumed that optical trapping becomes effective when the beam size is reduced to a certain value and the microparticles being trapped cannot escape out of the beam region. In this case, the optical trapping force is dominant and the other effects mentioned above are neglected. From Fig. 2, it is easily understood that the transmitted intensity will be enhanced or reduced at the focus point, depending on whether an ordered structure is achieved or not. Also, the recovery of the system to the initial state at the end of scanning is also clearly seen.

It should be emphasized here that the ordered structures formed in *Z*-scan trapping processes may exist in two different forms. One is a regular lattice of microparticles that do not contact with each other and the other is a close-packed structure. Obviously, optical binding plays a crucial role in the creation of ordered structures in the former case. In the latter case, it is thought that the gradient force is strong enough to hold the microparticles together. Based on the lattice constant derived from the diffraction pattern, we conclude that the microparticles in the ordered structures are nearly close packed with particle separation close to the diameter of particles. The detailed derivation of the lattice constant will be discussed elsewhere.

In experiments, we employed the conventional *Z*-scan

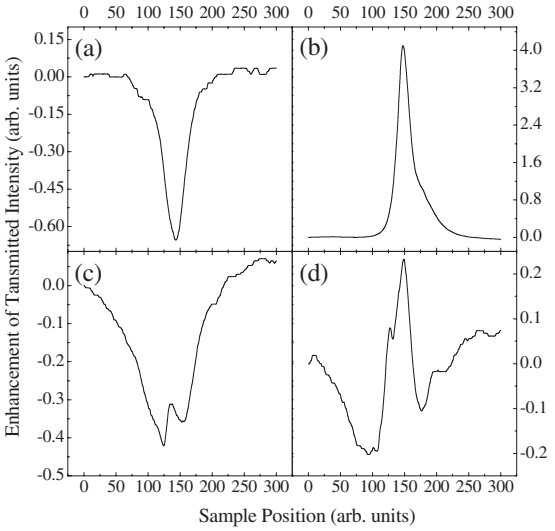

FIG. 3. (a) Disordered, (b) ordered, and [(c) and (d)] intermediate states in *Z*-scan-based trapping experiments.

technique to vary the beam size.[25,26] The arrangement is very similar to that for an open-aperture *Z*-scan experiment except that the detector was mounted on the same moving stage with the sample cell. The 532 nm light from a solid-state laser was used not only for trapping but also for detection. It was focused by using a 5× objective onto the sample cell. In most experiments, the scanning processes were performed in a region of $z \in (-d, +d)$ with $d=5.7625$ mm. The lowest scanning speed was set to be $v_0=191$ μm/s. The beam diameter was varied from ~2 mm at the two ends of the scanning to ~10 μm at the focus point. For microparticles, we chose monodisperse polystyrene (PS) and silica spheres purchased from Duke Scientific Corporation. The sample cell thickness was 50 μm. In our trapping experiments, the role of the scattering force is less important as compared to the gradient force because the confinement of the PS spheres in the z direction is provided by the two sidewalls of the sample cell.

III. DISORDERED, ORDERED, AND INTERMEDIATE STATES IN *Z*-SCAN TRAPPING EXPERIMENTS

Two distinct conditions, which represent a disordered state and an ordered one, respectively, are usually observed in *Z*-scan trapping experiments. They are characterized by the significant attenuation and enhancement of the transmitted intensity of the trapping light at the focus point, as shown in Fig. 3. For the sake of comparison, we use the relative enhancement of the transmitted intensity that is defined as $[I(z)-I_0]/I_0$ in all *Z*-scan traces. Here, $I_0=I(-d)$ is the transmitted intensity at the starting point of a *Z*-scan process. In addition, we define the enhancement factor for each *Z*-scan trace as $\eta=(I(0)-I_0)/I_0$, where $I(0)$ is the transmitted intensity at the focus point. As can be seen later, η can be used as a proxy measure for characterizing the quality of the formed structures. In the case of a disordered state, the number of PS spheres being trapped is not sufficient to form an ordered structure at the focus point [see Fig. 3(a)]. It means that the trapping region remains to be a disordered state at the focus point but with a higher concentration of PS spheres. Consequently, the trapping light suffers from a stronger scattering, resulting in a lower transmission. In the case of an ordered state, however, the number of PS spheres collected by the trapping light is adequate to fill the beam volume in a close-packed form. As a result, a phase transition from a disordered state to an ordered one occurs in the trapping region at the focus point, leading to a significant enhancement in the transmission of the trapping light [see Fig. 3(b)]. In other words, the trapping region becomes nearly transparent to the trapping light. Apparently, the gradient force, which can be varied by adjusting trapping power, plays an important role in triggering this phase transition. In experiments, the phase transition mentioned above does not occur sharply with increasing trapping power. As a result, we observed some intermediate states at trapping powers close to the threshold, as shown in Figs. 3(c) and 3(d). In these cases, a small peak appears at the focus point although the tendency of the transmitted intensity reduction close to the focus point remains unchanged. It indicates the onset of the phase transition. Sometimes, the intensity of the small peak may exceed the initial transmitted intensity, as can be seen in Fig. 3(d).

IV. QUALITY AND STABILITY OF THE FORMED ORDERED STRUCTURES

It has been shown that ordered structures can be achieved when the trapping power exceeds a threshold. In this case, the transmission valleys in *Z*-scan traces are replaced by transmission peaks. However, it does not imply that the higher the trapping power, the better the ordered structure. The physical reason is that the balance between the scattering force in the forward direction and the longitudinal component of the gradient force will be broken at high trapping powers. In this case, the convection of microparticles may occur, leading to the degradation of the quality of ordered structures. It has been revealed that the quality of the ordered structures exhibits a strong dependence on the trapping power for a sample cell in which the other parameters have been fixed. There exists an optimum trapping power at which an ordered structure with best quality is achieved. At the lowest scanning speed ($v_0=191$ μm/s), the optimum trapping power is determined to be ~50 mW.

The quality of the ordered structures formed in the *Z*-scan trapping experiments is characterized by examining either the enhancement of the transmitted intensity or the diffraction pattern of the trapping region. It is thought that the transparency of the ordered structures is governed by the volume density of the imperfections inside them. In other words, the enhancement of the transmitted intensity of the trapping light reflects the ordering of the formed structures. Thus, the enhancement factor defined above is considered to be a rough criterion for judging the quality of the formed structures. On the other hand, the ordering of the formed structures should be reflected in the diffraction pattern of the trapping region, as already addressed in Ref. 29. From the width of the diffraction peaks, we are able to determine the ordering of the formed structures. Here, we compare the *Z*-scan traces and the diffraction patterns for the ordered

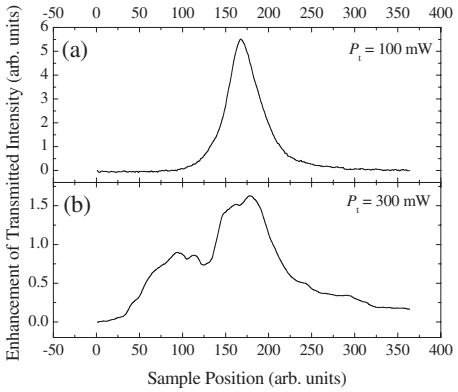

FIG. 4. *Z*-scan traces obtained at trapping powers of (a) P_t=100 mW and (b) P_t=300 mW.

structures obtained at two different trapping powers (P_t) of 100 and 300 mW, as shown in Figs. 4 and 5, respectively. It can be seen that the enhancement factor achieved at 100 mW (~5.5) is larger than that obtained at 300 mW (~1.8). Accordingly, the diffraction pattern observed at 100 mW looks much better than that recorded at 300 mW. For P_t =100 mW, well-defined diffraction spots are observed on a neat background. The widths of the diffraction peaks appear to be quite narrow. In contrast, the widths of the diffraction peaks are broadened significantly, and the background becomes noisy at P_t=300 mW.

As compared with other techniques, the *Z*-scan-based optical trapping exhibits great advantages in controlling the stability of the ordered structures. Consequently, the reversible feature of optical matters is clearly demonstrated by optimizing the experimental conditions, as evidenced in Fig. 6. The *Z*-scan traces for three consecutive scanning processes are presented together for comparison. A rest time of 5 min was inserted in two consecutive scanning processes. Evidently, no obvious difference is found in the three traces. It indicates that the ordered structures with nearly the same quality can be reproduced provided that the initial status is the same.

V. CONDITIONS FOR OBSERVING SELF-INDUCED TRANSPARENCY

The above experimental results were obtained by using a 50-μm-thick sample cell containing 1.9 μm diameter PS spheres with a concentration of 10%. As indicated above, the formation of ordered structures and the resulting transparency occur only when the beam volume at the focus point is completely filled with PS spheres. Therefore, ordered structures will not be achieved when using PS spheres with small diameters or thick sample cells. In order to verify the physical model presented in Sec. II, we have carried out *Z*-scan trapping experiments on systems with different parameters. Figure 7 shows the *Z*-scan traces obtained for a 50-μm-thick sample cell containing 260 nm diameter PS spheres at different trapping powers. In all cases, we observed an attenuation of the transmitted intensity at the focus point rather than an enhancement. It means that no ordered structure is formed even in the cases of high trapping powers. The *Z*-scan traces for a 200-μm-thick sample cell containing 1.9 μm diameter PS spheres at different trapping powers are shown in Fig. 8. In this case, the beam volume at the focus point is increased four times. Similarly, we did not observe the formation of ordered structures for all trapping powers that we used. It implies that the number of PS spheres being trapped is not sufficient to completely fill the beam volume in a close-packed form. These two examples clearly verify the physical model for the *Z*-scan-based optical trapping proposed by us in Sec. II.

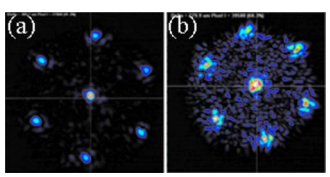

FIG. 5. (Color online) Diffraction patterns of the trapping region obtained at trapping powers of (a) P_t=100 mW and (b) P_t=300 mW.

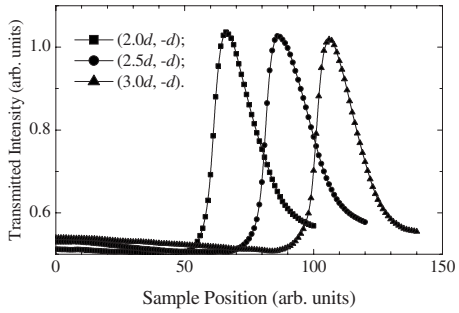

FIG. 6. Results of the *Z*-scan trapping experiments performed for different scanning ranges at a trapping power of 100 mW. For each curve, the peak corresponds to the focus point of the scanning process. The scanning ranges are indicated.

VI. SEQUENTIAL TRAPPING OF INDIVIDUAL MICROPARTICLES

When the diameter of PS spheres is small and the concentration is low, the trapping effect becomes less effective for large volume trapping. In this case, it is possible to ob-

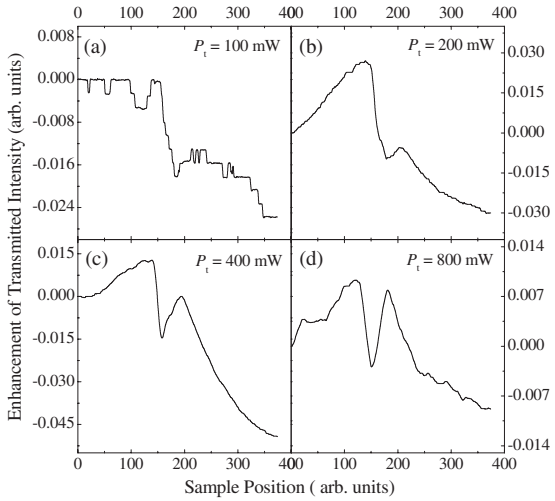

FIG. 7. *Z*-scan traces obtained at different trapping powers for a 50-μm-thick sample cell containing 260 nm PS spheres: (a) P_t=100 mW, (b) P_t=200 mW, (c) P_t=400 mW, and (d) P_t=800 mW.

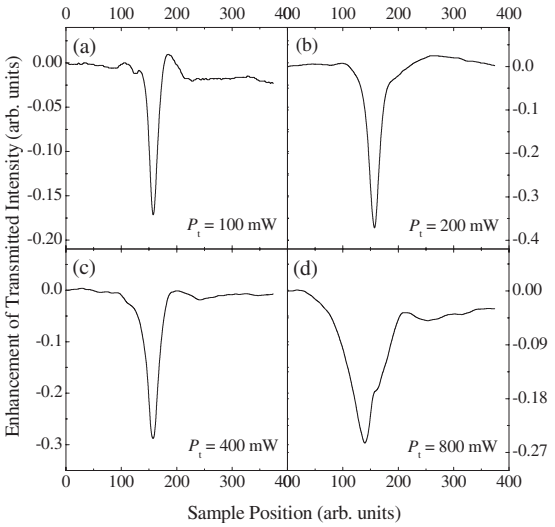

FIG. 8. *Z*-scan traces obtained at different trapping powers for a 200-μm-thick sample cell containing 1.9 μm PS spheres: (a) P_t=100 mW, (b) P_t=200 mW, (c) P_t=400 mW, and (d) P_t=800 mW.

serve the trapping of single particles or fewer in *Z*-scan trapping experiments. Similar phenomenon has been observed by Hosokawa *et al.*[30] by using luminescent PS spheres. In our case, although the PS spheres are not luminescent, we report the sequential trapping of individual PS spheres from the transmitted intensity in the trapping experiments. The sample cell that we used contains 260 nm PS spheres with a concentration of 1%. For trapping powers lower than 10 mW, the gradient force exerted on PS spheres is quite small because it is proportional to the third power of the particle diameter. Thus, the trapping event occurs occasionally in the scanning process, which is manifested in the decrease in the transmitted intensity, as shown in Fig. 9(a). Meanwhile, the PS spheres may have a chance to escape out of the optical potential if the thermal kinetic energy is greater than the

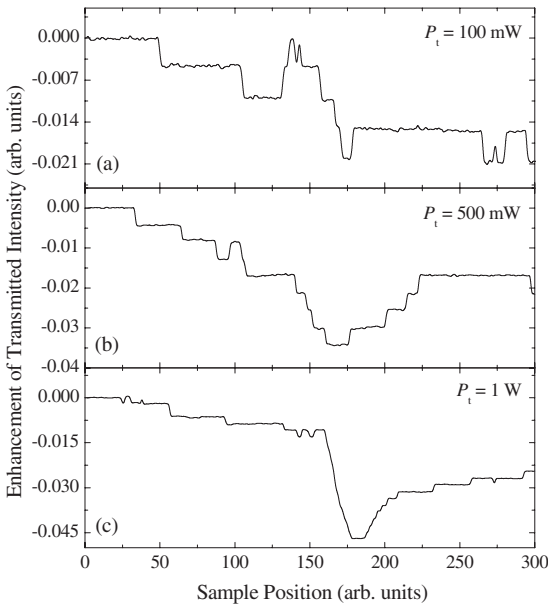

FIG. 9. *Z*-scan traces obtained at different trapping powers for a 50-μm-thick sample cell containing 260 nm PS spheres of 1 wt %: (a) P_t =100 mW, (b) P_t=500 mW, and (c) P_t=1 W.

barrier height. This behavior is reflected in the increase in the transmitted intensity. It is noticed that the decrease or increase in the transmitted intensity is almost a constant, similar to that reported by Hosokawa *et al.*[30] by monitoring the photoluminescence. It implies that the *Z*-scan-based optical trapping can also be employed to study the trapping of single particles. With increasing trapping power, the trapping events occur frequently and the steps appear to be short in the traces, as shown in Fig. 9(b). Finally, the trapping of single particles cannot be distinguished at high trapping powers [see Fig. 9(c)].

VII. MULTIPLE TRAPPING PROCESSES

In the previous work, we have demonstrated the phase transition from a disordered state to an ordered one in a single *Z*-scan trapping process.[27] It is manifested in a significant enhancement of the transmitted intensity of the trapping light. Such a transition occurs when the number of PS spheres being trapped is adequate to completely fill the beam volume in a close-packed form. It has been shown that the phase transition does not occur at low trapping powers because the number of PS spheres collected by the trapping light is insufficient. However, the PS spheres within the effective trapping volume are driven quickly to the beam center when the sample cell approaches the focus point. As a result, a ring-shaped depletion region is formed, as shown in Fig. 2(d). After the sample cell passes through the focus point, the beam size is enlarged. In this case, the PS spheres both inside and outside the depletion region will be driven toward the depletion region by both gradient force and normal diffusion. However, it generally takes some time for the PS spheres to reach their initial distribution. If we perform the next scanning process immediately without giving the sample cell a rest time, then the number of PS spheres within the effective trapping region will increase. Therefore, it is expected that the phase transition in the trapping region can be realized by performing a multiple trapping process without any interruption. In the multiple trapping process, more and more PS spheres are attracted to the beam center by gradient force, and eventually a phase transition should occur. Depending on the diameter and concentration of PS spheres, several tens of consecutive trapping processes may be needed to realize the phase transition. As an example, we show a multiple trapping process containing 30 consecutive *Z*-scan trapping processes. Some typical traces are presented in Fig. 10. While the initial and final states are characterized by a transmission valley and a transmission peak at the focus point, the intermediate states generally appear to be quite different.

In Figs. 10(a) and 10(b), a deep attenuation of the transmitted intensity at the focus point is clearly observed. The increase in the trapped PS spheres in the beam region is responsible for this behavior. It is noticed that the attenuation of the transmitted intensity at the focus point becomes smaller after several trapping processes, as shown in Figs. 10(c) and 10(d). In Figs. 10(e) and 10(f), a tiny peak appears at the focus point, although the tendency of the transmitted intensity reduction remains unchanged. From Fig. 10(g) to

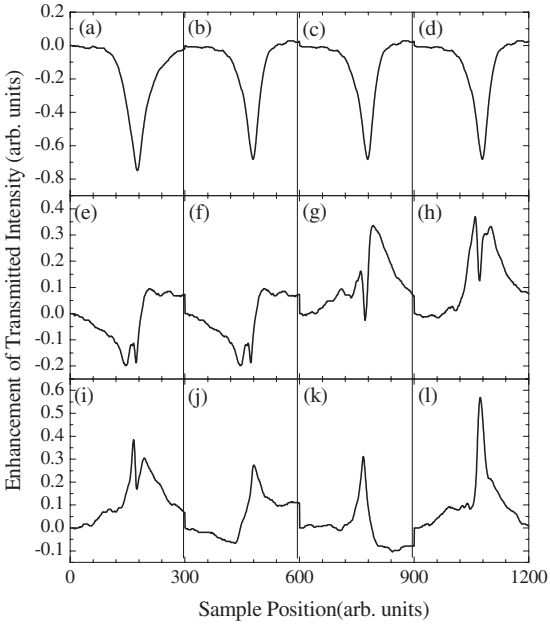

FIG. 10. *Z*-scan traces observed in different scanning processes in a multiple trapping process.

Fig. 10(i), we observe an increase in the transmitted intensity when the sample cell approaches the focus point. However, a small dip in transmittance appears at the focus point. In Figs. 10(j)–10(l), an enhancement in the transmitted intensity is clearly observed at the focus point, indicating the formation of an ordered structure. With the increasing number of scanning processes, the enhancement factor also increases.

The transition from a disordered state to an ordered one by utilizing a multiple trapping process is clearly reflected in the change in the enhancement factor, which has been defined in Sec. III. In Fig. 11, we present the evolution of the enhancement factor with increasing number of trapping process. It can be seen that the enhancement factor is increased from −0.75 to 0.57 after 30 consecutive trapping processes.

VIII. DEPENDENCE OF TRAPPING BEHAVIOR ON SCANNING SPEED AND TRAPPING POWER

It has been shown that the phase transition from a disordered state to an ordered one can be induced by simply increasing the trapping power. The increase in trapping power will lead to an increase in the gradient force exerted on PS spheres and thus the increase in the collection efficiency of

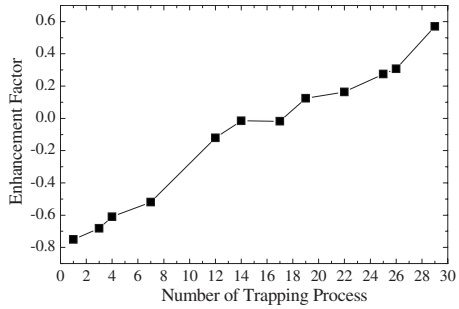

FIG. 11. Evolution of the enhancement factor observed in a multiple trapping process.

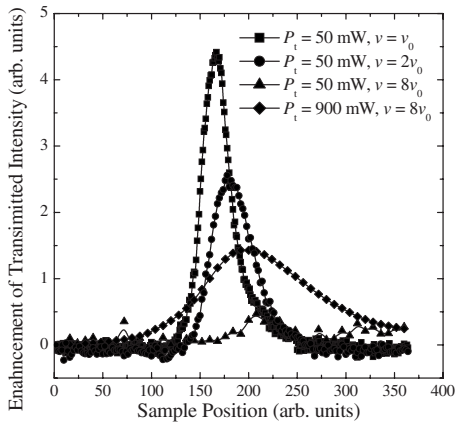

FIG. 12. Dependence of *Z*-scan trace on scanning speed and trapping power.

PS spheres during the scanning process. Apparently, another parameter that affects the trapping efficiency of PS spheres is scanning speed. The experimental results described above were performed at the lowest scanning speed of $v_0 = 191\ \mu\text{m/s}$. If we increase the scanning speed, it is expected that the interaction time between light and PS spheres is reduced. As a result, some PS spheres may not be able to catch up with the movement of the laser beam, resulting in a lower trapping efficiency. In Fig. 12, we show the evolution of the *Z*-scan trace with increasing scanning speed. It can be seen that the enhancement factor decreases rapidly with increasing scanning speed. At the highest speed that we used in trapping experiments ($v = 8v_0$), no obvious enhancement is observed. This behavior also confirms the physical model for *Z*-scan-based optical trapping. By raising the trapping power, however, it is expected that we can compensate the reduction in trapping efficiency caused by increasing the scanning speed. Consequently, we can see that the enhancement in transmitted intensity at the focus point is observed again at a trapping power of 900 mW. It means that the total momentum transferred from photons to PS spheres, which determines the trapping efficiency, depends not only on the gradient force but also on the interaction time. These two quantities can be adjusted by changing the trapping power and scanning speed.

IX. DEPENDENCE OF TRAPPING BEHAVIOR ON PARTICLE SIZE AND MATERIAL

In Sec. V, we have showed that the phase transition does not occur when using small PS spheres of 260 nm diameter. It is ascribed to the gradient force that is proportional to the third power of the diameter of PS spheres. Therefore, the gradient force is expected to decrease by about three orders of magnitude when the diameter of PS spheres is reduced from 1.9 μm to 260 nm. In Fig. 13, we compare the *Z*-scan traces for PS spheres with different diameters of 260 nm, 1.9, 4.3, and 10 μm at a trapping power of 100 mW. In Fig. 13(a), no enhancement of transmitted intensity is observed for 260 nm PS spheres. For PS spheres of 1.9 and 4.3 μm diameter, an enhancement of transmitted intensity is observed at the focus point. However, the 4.3 μm diameter PS spheres exhibit a larger enhancement factor as compared

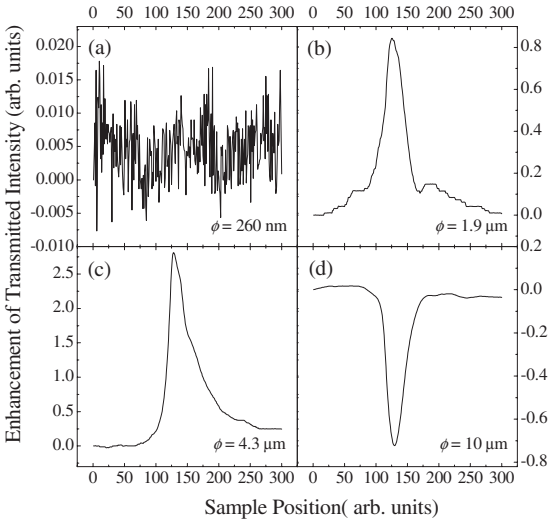

FIG. 13. Dependence of *Z*-scan trace on the diameter (ϕ) of PS spheres: (a) ϕ=260 nm, (b) ϕ=1.9 μm, (c) ϕ=4.3 μm, and (d) ϕ=10 μm.

with the 1.9 μm diameter ones because the relatively larger gradient force results in a higher trapping efficiency. Surprisingly, a transmission valley is found in the *Z*-scan trace for the 10 μm diameter PS spheres, as shown in Fig. 13(d). We think that two reasons are responsible for this behavior. First, the 10 μm diameter PS spheres are too heavy to be uniformly distributed in water, which affects significantly the trapping efficiency. Second, the uniformity of the 10 μm PS spheres available commercially is not as good as the smaller PS spheres. Therefore, it is difficult to induce a phase transition in such a colloidal liquid.

Before summarizing our research work, let us examine the influence of the material of particles on the trapping behavior. Figure 14 shows the *Z*-scan traces for 1.9 μm PS spheres and 1.6 μm silica spheres. It is noticed that under the same trapping power an enhancement is observed for PS spheres, while an attenuation is found for silica ones. Apparently, the major difference between these two types of particles is the material from which spheres are made. Although the diameter of silica spheres is slightly smaller than that of PS spheres, they are heavier than PS spheres. The larger mass of silica spheres may cause smaller trapping efficiency. In addition, it is suspected that the much larger nonlinear

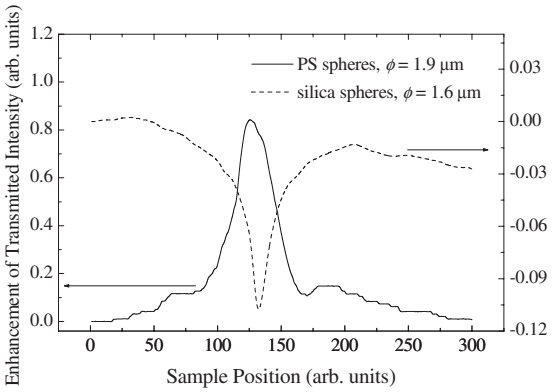

FIG. 14. Dependence of *Z*-scan trace on the material of microparticles: (a) 1.9 μm diameter PS spheres and (b) 1.6 μm diameter silica spheres.

coefficient of PS spheres as compared to silica ones may play an important role in determining the trapping efficiency. However, further experiments are needed to clarify this issue.

X. CONCLUSION

In summary, we have carried out a systematic study on the manipulation of microparticles in colloidal liquids by utilizing *Z*-scan-based optical trapping. A clear physical picture for *Z*-scan-based optical trapping has been established theoretically and verified experimentally. This technique is confirmed to be a simple and effective way to manipulate a large number of microparticles and to form ordered structures with good quality and stability. The dependence of the quality of the formed structures on trapping power and scanning speed is clarified, and the influence of the size and material of the particles is discussed. This technique has offered us an opportunity to observe the continuous transition from a disordered state to an ordered one. The dynamical ordered structures formed in this way may find applications in the construction of functional devices.

ACKNOWLEDGMENTS

The authors acknowledge the financial support from the National Natural Science Foundation of China (Grant Nos. 10674051 and 10811120010), the Natural Science Foundation of Guangdong province of China (Grant No. 06025082), and the Program for Innovative Research Team of the Higher Education in Guangdong (Grant No. 06CXTD005).

[1] A. Ashkin, Phys. Rev. Lett. **24**, 156 (1970).
[2] A. Ashkin, J. M. Dziedzic, J. E. Bjorkholm, and S. Chu, Opt. Lett. **11**, 288 (1986).
[3] M. P. MacDonald, L. Paterson, K. Volke-Sepulveda, J. Arlt, W. Sibbett, and K. Dholakia, Science **296**, 1101 (2002).
[4] T. Sugiura, T. Okada, Y. Inouye, O. Nakamura, and S. Kawata, Opt. Lett. **22**, 1663 (1997).
[5] S. Ito, H. Yoshikawa, and H. Masuhara, Appl. Phys. Lett. **78**, 2566 (2001).
[6] R. C. Gauthier, M. Ashman, and C. P. Grover, Appl. Opt. **38**, 4861 (1999).
[7] J. N. Wilking and T. G. Mason, Europhys. Lett. **81**, 58005 (2008).
[8] S. Sato, Y. Harada, and Y. Waseda, Opt. Lett. **19**, 1807 (1994).
[9] H. Furukawa and I. Yamaguchi, Opt. Lett. **23**, 216 (1998).
[10] T. Iida and H. Ishihara, Phys. Rev. Lett. **90**, 057403 (2003).
[11] A. Chowdhury, B. J. Ackerson, and N. A. Clark, Phys. Rev. Lett. **55**, 833 (1985).
[12] M. M. Burns, J.-M. Fournier, and J. A. Golovchenko, Phys. Rev. Lett. **63**, 1233 (1989).
[13] M. M. Burns, J.-M. Fournier, and J. A. Golovchenko, Science **249**, 749 (1990).
[14] S. A. Tatarkova, A. E. Carruthers, and K. Dholakia, Phys. Rev. Lett. **89**, 283901 (2002).
[15] E. Yablonovitch, Phys. Rev. Lett. **58**, 2059 (1987).
[16] S. John, Phys. Rev. Lett. **58**, 2486 (1987).
[17] J. D. Joannopoulos, R. D. Meade, and J. N. Winn, *Photonic Crystals: Molding the Flow of Light* (Princeton University Press, Princeton, New Jersey, 1995).
[18] *Photonic Crystals: Physics, Fabrication, and Applications*, edited by K. Inoue and K. Ohtaka (Springer-Verlag, Berlin, 2004).
[19] E. R. Dufresne and D. G. Grier, Rev. Sci. Instrum. **69**, 1974 (1998).
[20] D. G. Grier, Nature (London) **424**, 810 (2003).
[21] R. Eriksen, V. Daria, and J. Glückstad, Opt. Express **10**, 597 (2002).

[22]H. Melville, G. Milne, G. Spalding, W. Sibbett, K. Dholakia, and D. McGloin, Opt. Express **11**, 3562 (2003).
[23]J. Leach, G. Sinclair, P. Jordan, J. Courtial, M. Padgett, J. Cooper, and Z. Laczik, Opt. Express **12**, 220 (2004).
[24]D. G. Grier and Y. Roichman, Appl. Opt. **45**, 880 (2006).
[25]M. Sheik-Bahae, A. A. Said, and E. W. Van Stryland, Opt. Lett. **14**, 955 (1989).
[26]M. Sheik-Bahae, A. A. Said, T.-H. Wei, D. J. Hagan, and E. W. Van Stryland, IEEE J. Quantum Electron. **26**, 760 (1990).
[27]Q.-F. Dai, H.-Y. Liu, J. Liu, L.-J. Wu, Q. Guo, W. Hu, X.-B. Yang, S.-H. Liu, S. Lan, A. V. Gopal, and V. A. Trofimov, Appl. Phys. Lett. **92**, 153111 (2008).
[28]T. M. Grzegorczyk, B. A. Kemo, and J. A. Kong, Phys. Rev. Lett. **96**, 113903 (2006).
[29]S. Förster, A. Timmann, C. Schellbach, A. Frömsdorf, A. Kornowski, H. Weller, S. V. Roth, and P. Lindner, Nature Mater. **6**, 888 (2007).
[30]C. Hosokawa, H. Yoshikawa, and H. Masuhara, Phys. Rev. E **70**, 061410 (2004).